AlCoCrCuFeNi-Based High-Entropy Alloys: Correlation Between Molar Density and Enthalpy of Mixing in the Liquid State

YURIY PLEVACHUK, JÜRGEN BRILLO, and ANDRIY YAKYMOVYCH

The density of the liquid equiatomic high-entropy alloys, namely, AlCoCrCuFeNi, AlCoCuFeNi, and CrCoCuFeNi, as well as quaternary alloys AlCoCuFe and AlCoCrNi was determined over a wide temperature range. The measurements were performed by a non-contact technique combining electromagnetic levitation and optical dilatometry. The temperature and composition dependencies of the density were analyzed and the molar excess volumes were calculated. The integral enthalpy of mixing of multi-component alloys was predicted using extended Kohler's model, while Miedema's model was used for binary sub-system alloys. It has been found that a negative excess volume of the investigated Al-containing liquid alloys correlates with a negative enthalpy of mixing. In contrast, a positive excess volume and an endothermic reaction have been estimated for the liquid CoCrCuFeNi alloy. The change of the excess volume in the Al-containing liquid alloys is affected by two basic effects, namely, compression of the Al matrix and formation of compounds in the melt.

https://doi.org/10.1007/s11661-018-4925-4

I. INTRODUCTION

CONVENTIONAL alloys are mainly based on one principal element with different kinds of alloying elements added to improve their properties. These alloys form an alloy family based on the chosen principal element. However, the number of elements in the periodic table is limited, and thus the alloy families, which can be developed, are also limited. The new concept, first proposed in 1995, has been named a high-entropy alloy (HEA).[1,2] According to proposed definition, any multi-component alloy consisting of five or more principal elements, which have a concentration between 5 and 35 at. pct, belongs to the HEA family. Besides principal elements, HEAs could contain also minor elements with concentrations below 5 at. pct.

Compared to conventional alloys, these alloys have significantly higher mixing entropies, which lead to the formation of liquid or random solid solution states.[3,4] Thus, the effect of entropy is much more pronounced in HEAs than in conventional alloys. According to the Gibbs phase rule, a system of i components could contain maximum $(i + 1)$ phases in the equilibrium state. The experimental results published in References 4 and 5 show that the high entropy of mixing in these alloys facilitates the formation of solid solution phases with simple structures. Thus, it reduces the number of phases formed in HEAs during solidification process. Such unique structural features caused by the effect of higher entropy are of paramount importance for further industrial application of these alloys.[6]

Due to the unique multi-principal element composition, HEAs can possess extraordinary properties, including high strength/hardness, outstanding wear resistance, exceptional high-temperature strength, good structural stability, good corrosion, and oxidation resistance. Some of these properties are not seen in conventional alloys, making HEAs attractive in many fields. The fact that it can be used at high temperatures broadens its spectrum of applications even further. Moreover, a fabrication of HEAs does not require special processing techniques or equipment, which indicates that the mass production of HEAs can be easily implemented with existing equipment and technologies. According to Reference 4, more than 300 HEAs have been reported, which were prepared from more than 30 various elements. Based on the above

YURIY PLEVACHUK is with the Department of Metal Physics, Ivan Franko National University of Lviv, 79005 Lviv, Ukraine. Contact e-mail: plevachuk@mail.lviv.ua JÜRGEN BRILLO is with the Institut für Materialphysik im Weltraum, Deutsches Zentrum für Luft- und Raumfahrt (DLR), 51170 Cologne, Germany. ANDRIY YAKYMOVYCH is with the Department of Metal Physics, Ivan Franko National University of Lviv and also with the Department of Inorganic Chemistry – Functional Materials, Faculty of Chemistry, University of Vienna, 1090 Vienna, Austria. Contact e-mail: andriy.yakymovych@univie.ac.at

Manuscript submitted March 6, 2018.
Article published online September 24, 2018

mentioned, we have a new rapidly developing class of metallic materials.

The development of new advanced materials with predicted properties requires a clear and thorough understanding of their structural properties on the basis of sufficient and reliable thermophysical data. The increasing influence of computational modeling in all technological processes generates an increased demand for accurate values of the physical properties of the materials involved, which are used as fundamental inputs for each model. The solidification process of a liquid alloy has a profound impact on the structure and properties of the solid material. Therefore, knowledge of the thermophysical properties of molten alloys becomes very important for understanding the structural transformations in alloys in the liquid–solid temperature range and modeling of the solidification process, so that materials with required characteristics can be developed.

The density as one of the thermophysical structure-sensitive properties plays an important part in solidification. For example, the density gives essential information for reliable simulation of various industrial metallurgical processes. The molar volume and the excess molar volume are obtained from the experimental data of the density. It should be noted that the excess molar volume is one of the key mixing parameters. Unfortunately, there is no general rule of thumb whether or not it is positive, negative, or zero. However, it is found that strongly mixing systems with negative excess Gibbs energy tend to exhibit a negative excess volume, while demixing systems with positive excess Gibbs energy show a negative excess volume. For alloys which consist of chemically similar components, the excess volume is almost zero.[7,8]

The main goal of the present study was to receive a set of reliable thermophysical data (density, molar volume) of the liquid phase of selected HEAs. The equiatomic AlCoCrCuFeNi high-entropy alloy (corresponds to $Al_{16.6}Co_{16.6}Cr_{16.6}Fe_{16.6}Ni_{16.6}$ in at. pct) and its four- and five-component sub-system alloys with equiatomic compositions were chosen for the present research. It is important to know, if the excess molar volume indicated in ternary sub-system alloys[9,10] would disappear with the increasing number of the alloy components. It is supposed that the increasing temperature leads to the vanishing of excess properties due to larger value of the entropy, when chemical interactions between atoms became overcome. In the case of high-entropy alloys, a higher value of entropy is achieved by increasing the numbers of components.

Furthermore, a correlation between excess molar volume and the integral enthalpy of mixing has been examined. For this reason, the integral enthalpy of mixing was calculated based on the data for binary sub-systems. Since no experimental literature values are available for Co-Cr and Cr-Cu alloys, the corresponding integral enthalpy of mixing was estimated using Miedema's semi-empirical model.[11] The corresponding calculations for studied multi-component alloys were performed by extending the thermodynamic geometrical model of Kohler, using either calculated or experimental data for the enthalpies of mixing of binary sub-system alloys. Furthermore, the characteristic temperatures of the alloys were determined by differential thermal analysis (DTA). The obtained experimental results were compared with literature data. Such a data set allows for a quantitative simulation of casting multi-component alloys.

II. EXPERIMENTAL

The experiments were carried out with an electromagnetic levitation (EML) facility designed for optical dilatometry (OD).[12] The samples were positioned and melted by electromagnetic fields. The sample volume was measured by a shadow-graph technique in a parallel expanded laser beam as described in Reference 13. The sample temperature was measured with an infrared pyrometer. The temperature was recalibrated for each sample with respect to the liquidus temperature taken from differential thermal analysis (DTA), described below, using an approximation derived from Wien's law as explained in Reference 7. The temperature was regulated by carefully cooling the sample in a laminar flow of Ar or He gas, which was admitted from below *via* a ceramic tube. The resultant accuracy in the pyrometric measurements is ± 10 to 15 K.

The samples were prepared by arc-melting of the proper amounts of pure metals provided by the company Alfa Aesar, namely, Al (99.999 pct), Co (99.995 pct), Cr (99.995 pct), Cu (99.995 pct), Fe (99.995 pct), and Ni (99.999 pct). Prior to the measurement, each sample was melted in the levitation process in order to get a homogeneous alloy. Then the surface of the solidified sample was cleaned mechanically and rinsed with propanol. The samples were always first heated up to the highest experimental temperature and then measurements were started. After measuring one data point the temperature was decreased by 10 to 20 K and the next data point was taken.

Processing of the selected alloys in the liquid phase poses experimental difficulties due to a large difference in the melting temperature of Al to other constituents. It was supposed that Al could evaporate during measurements leading to a shift in the sample composition and to contamination of the optical path. Therefore, several samples with similar composition were measured in order to exclude a possible deviation in density values. Furthermore, each sample was weighed before and after the experiments. If a sample lost more than 0.1 pct of its initial mass, the measurement was excluded. The total error for the density measurements is estimated in Reference 12 to be $\Delta\rho/\rho \approx 1$ pct. Whereas the error in the mass, $\Delta m/m$, is of the order of 0.1 pct, the major source of error comes from the determination of the volume, $\Delta V/V$, and is due to the calibration of the digital images, which is of the order of 1 pct. The error in temperature is due to the uncertainty of the temperature dependence of the emissivity, and is estimated to be of the order of 5-10 K.

The DTA measurements were carried out by a Netzsch DTA 404 PC (Netzsch, Selb, Germany) under a constant Ar flow of 50 mL min^{-1} using alumina

crucibles (Al_2O_3) with a cover. The measurements were performed in two runs with a heating rate of 5 K min^{-1}. Two heating and cooling curves were recorded for each sample to check reproducibility of thermal effects afterwards. The samples weighed around 100–110 mg and a possible mass loss during the DTA investigations was checked routinely. No relevant mass changes were observed.

III. CALCULATION

A. *Kohler's Model*

There are a number of papers dealing with an attempt to extend Miedema's approach to multi-component systems.[14–21] In most of these works, the main approach was to calculate the enthalpy of formation of a ternary system as a sum of enthalpies of respective binary sub-systems.[14–16] For instance, Gallego *et al.*[14] proposed a following equation to calculate the enthalpy of mixing of the ternary alloy, $\Delta^{\text{chem}}H_{ABC}$:

$$\Delta^{\text{chem}}H_{ABC} = \Delta H^{\text{chem}}_{AB} + \Delta H^{\text{chem}}_{BC} + \Delta H^{\text{chem}}_{AC}, \quad [1]$$

where $\Delta^{\text{chem}}H_{AB}$, $\Delta^{\text{chem}}H_{BC}$, and $\Delta^{\text{chem}}H_{AC}$ are the enthalpies of mixing of sub-binary *A-B*, *B-C*, and *A-C* alloys, respectively.

In this paper, the integral enthalpy of mixing of multi-component alloys was calculated based on the corresponding values for binary sub-system alloys using Kohler's model[22] extended for multi-component systems. According to Kohler's model, the interaction parameters between two specific components in a multi-component alloy are not affected by other components.[22] Therefore, the enthalpy of mixing of a multi-component alloy, $\Delta_{\text{mix}}H$, is equal to a sum of their binary sub-system alloys and can be rewritten as

$$\Delta_{\text{mix}}H = \sum_i \sum_{j>i} (x_i + x_j)^2 \Delta_{\text{mix}}H_{ij}\left(\frac{x_i}{x_i + x_j}; \frac{x_j}{x_i + x_j}\right), \quad [2]$$

where x_i and x_j are the atomic concentrations of components *i* and *j*, respectively; $\Delta_{\text{mix}}H_{ij}$, is the enthalpy of mixing of the binary *i-j* system.

B. *Miedema's Model*

The integral enthalpy of mixing of binary sub-system alloys was calculated using Miedema's model. The "macroscopic atoms" model proposed by Miedema is one of the most widely used approaches to predict changes in the enthalpy of binary metal alloys. This semi-empirical theory is based on the concept of atomic cells requiring data of pure components. The heat effects caused by interactions of atoms of dissimilar elements affect the electron density at the boundary of the Wigner–Seitz (n_{ws}) cell and tend to shift their electron densities due to the electronegativity difference. These two main features of the model can be expressed as[23]

$$(n_{\text{ws}})^2 = K/V, \quad [3]$$

$$\phi^* = 5.2(Z/V)^{1/3} + 0.7 \text{ for non-transition metals}, \quad [4]$$

$$\phi^* = 5.2(Z/V)^{1/3} + 0.2 \text{ for transition metals}, \quad [5]$$

where V is the molar volume; K is the bulk modulus; Z is the number of valence electrons per atom; ϕ^* is the chemical potential charge of components or the work function of the pure metal readjusted to alloying behavior.

It is supposed that the enthalpy of the chemical mixing required for solving one mole of a component *A* in a component *B* is equal to

$$\Delta H^{\text{chem}}_{A \text{ in } B} = \Delta H^{\text{sol}}_{A \text{ in } B} = \frac{2 \cdot V_A^{2/3}}{\left[\left(n^A_{\text{ws}}\right)^{-1/3} + \left(n^B_{\text{ws}}\right)^{-1/3}\right]} \times \left(-P(\Delta\phi^*)^2 + Q\left(\Delta n^{1/3}_{\text{ws}}\right)^2 - R\right), \quad [6]$$

where P, Q, and R are the proportionality constants; $\Delta n^{1/3}_{ws}$ is the electron-density discontinuity equal to $(n^A_{\text{ws}})^{1/3} - (n^B_{\text{ws}})^{1/3}$; $\Delta\phi^*$ is the electronegativity difference defined as $\phi_A - \phi_B$ and V_A is the molar volume of the component *A*. The values of the fitting parameters P, Q, and R can be determined from tables proposed in References 23 and 24.

The integral enthalpy of mixing of binary A–B system can be written as

$$\Delta_{\text{mix}}H_{AB} = \Delta H^{\text{chem}}_{AB} = x_A \cdot x_B \cdot \left(x^s_B \Delta H^{\text{chem}}_{A \text{ in } B} + x^s_A \Delta H^{\text{chem}}_{B \text{ in } A}\right), \quad [7]$$

where x_A and x_B are the atomic concentrations of the components *A* and *B*, respectively; x^S_A and x^S_B denote, respectively, concentration ratios of atoms *A* and *B* in the surface. The concept of surface concentration was introduced to take into account the total area of the contact surface between dissimilar atoms related with a change in boundary conditions when an atomic cell is transferred from a pure metal to an alloy.

The mole fraction of the component *A* on the surface is given as

$$x^s_A = 1 - x^s_B = \frac{x_A V_A^{2/3}}{x_A V_A^{2/3} + x_B V_B^{2/3}}. \quad [8]$$

The values of the molar volumes of the components were calculated or taken from the literature data of density.[9,25–28] It should be noted that Eq. [7] is applied for alloys without chemical short-range order in the structure.

IV. RESULTS AND DISCUSSION

A. *Modeled Enthalpy of Mixing*

The calculated values of the enthalpy of mixing of binary sub-system alloys at 1700 K are presented in Table I and compared therein with literature data. In our calculations, it is suggested that several binary sub-system alloys with the liquidus temperature above 1700 K are in a virtual metastable liquid state. This means that they are assumed liquid, although the temperature of 1700 K is below their liquidus. These alloys are marked with asterisks in Table I. The literature data for most binary alloys were estimated from calorimetric experiment, except CoCr and CrCu. The thermodynamic excess functions of liquid Co-Cr alloys in the concentration range between 27.2 and 60.5 at. pct Cr were estimated based on the Knudsen-cell mass spectrometric measurements.[29] The partial and integral enthalpies of mixing of the Cr-Cu system were calculated in Reference 30, based on experimental values of the dissolution enthalpy of Cr in Cu at 1873 K, taken from Reference 31.

Table II contains the values of the integral enthalpy of mixing of the multi-component alloys calculated by Kohler's model, based on either Miedema's model or on literature values for binary sub-systems.

As follows from Tables I and II, values of the integral enthalpy of mixing of binary sub-system alloys calculated using Miedema's model and their experimental data have the same sign and similar magnitude. This is also true for the multi-component alloys where $\Delta_{mix}H$ is determined using Kohler's model. The only exception is CoNi. However, there is the relative small difference in values between the slightly negative value of -0.3 kJ mol^{-1} calculated by Eq. [11] and positive one of 0.4 kJ mol^{-1}, reported in the literature.[39] According to data from Table I, a more exothermic or less endodermic behavior was experimentally obtained for most presented binary alloys as compared with predictions of Miedema's model. A similar tendency was obtained for calculated $\Delta_{mix}H$ of the Al-Co-Cr-Cu-Fe-Ni alloys (Table II). The largest deviation between calculated data for multi-component alloys is obtained for AlCoCuFe and is equal to about 7.5 kJ mol^{-1}. It should be noted that a disagreement in experimental values of the integral enthalpy of mixing published for some systems by different authors could also reach 6 kJ mol^{-1}. For instance, according to El Khasan *et al.*,[42] $\Delta_{mix}H$ of the liquid Cu-Fe alloy is equal to 12.4 ± 1.3 kJ mol^{-1}, while a value of 6.78 kJ mol^{-1} at 1823 K was reported by Turchanin.[43]

The calculated heat effects for the studied multi-component alloys are in a good agreement with literature data,[44,45] for instance, with 3.20 kJ mol^{-1} for CoCrCuFeNi and -4.78 kJ mol^{-1} for AlCoCrCuFeNi calculated based on Miedema's model as well as 2.4 kJ mol^{-1} for the CoCrCuFeNi alloy determined at 1700 K using Muggianu's model.[46] Furthermore, an excellent agreement between values of the enthalpy of mixing for the Co$_x$CrCuFeNi alloys calculated using Miedema's and three thermodynamic geometrical models, namely, Kohler's, Muggianu's, and Chou's approaches, was shown by Arslan and Dogan.[46]

B. *Density Investigations*

Temperature dependence of the density, $\rho(T)$, of investigated alloys is presented in Figure 1. The highest values of the density were obtained for the alloy without aluminum, while the lowest values were revealed in quaternary liquid AlCoCrFe and AlCoCuNi alloys. As an overall trend, it is observed that the density of the investigated AlCoCrCuFeNi HEAs increases with increasing amount of the heavier metal.

Apart from a few abnormal systems, such as Si or water, the density in the liquid state can be approximated as a function of temperature by the following linear law, which holds over a wide temperature range[47]:

$$\rho(T) = \rho_L + \rho_T(T - T_L), \qquad [9]$$

where ρ is the density in (kg m^{-3}); T is the temperature in (K); ρ_L is the density in (kg m^{-3}) at the liquidus temperature, T_L; and ρ_T is the temperature coefficient in (K^{-1}) and (kg m^{-3}), respectively. Due to the indicated undercooling effect, the liquidus points were taken as a maximum of the peak from the heating DTA curves. As it is seen from Table III, the liquidus temperatures obtained from DTA measurements are in a good agreement with literature data,[5] indicating T_L equals 1603 K for the AlCoCrCuFeNi alloy, as well as 1662 K for the CoCrCuFeNi alloy.

As obvious from Figure 1, Eq. [9] is also fulfilled for the systems studied in the present work. The fitted parameters, ρ_L and ρ_T, are presented in Table IV. The molar volume of the liquid multi-component alloy can be calculated as

$$V = \sum_i x_i \frac{M_i}{\rho_i} + V^E, \qquad [10]$$

where V is the molar volume of the alloy; x_i, M_i, and ρ_i are the concentration, molar mass, and density of a component i; V^E is the excess molar volume. Due to high melting temperature of the employed transition metals, such as Co, Cr, Fe, and Ni, it was decided to perform calculations of the ideal volumetric mixing of the alloys referred to Vegard's law ($^{id}V = \sum_i x_i \frac{M_i}{\rho_i}$)[48] in a temperature interval ($T_L < T < 1728$ K) assuming that the density of pure components is equal to the value at the melting temperature of a corresponded metal, T_L^i, except Al and Cu.

As seen from Figure 2, the investigated liquid multi-component alloys have negative deviations in the molar volume. The only exception was determined for CoCrCuFeNi. According to literature data related to the molar volume measurements of liquid binary metal alloys,[49] strong negative deviations of this quantity are indicated in systems with chemical compounds in the solid state, while positive values of the excess molar volume were often reported for systems with a solid solution. Furthermore, the excess volumes of the liquid

Table I. Integral Enthalpy of Mixing for Binary Sub-System Alloys of the AlCoCrCuFeNi Alloy

Alloy	$\Delta_{mix}H$, kJ·mol^{-1} Eq. [11]	$\Delta_{mix}H$, kJ mol^{-1} (lit. data)	Source
AlCo	− 23.9*	− 32.1	32; 1873 K
AlCr	− 12.9*	− 7.03 ± 0.20	33; 1723 K
AlCu	− 9.6	− 13.1	34; 1723 K
AlFe	− 14.3	− 20.6	35; 1873 K
AlNi	− 28.5*	− 49.1*	36; 1773 K
CoCr	− 5.0	− 3.0	29; 1800 K
CoCu	7.2	7.03 ± 0.99	37; 1823 K
CoFe	− 0.6*	− 2.56	38; 1873 K
CoNi*	− 0.3	0.4	39; 1780 K
CrCu*	14.2	16.0	30; 1873 K
CrFe	− 1.6*	− 4.1*	40; 1873 K
CrNi	− 7.5	− 2.78 ± 0.23	33; 1729 K
CuFe	14.6	10.62 ± 0.90	37; 1873 K
CuNi	4.0	3.73 ± 0.58	37; 1753 K
FeNi	− 1.7*	− 4.4	41; 1753 K

*In virtual metastable liquid state.

Table II. Integral Enthalpy of Mixing for the Studied Liquid Alloys

Alloy Composition	$\Delta_{mix}H$, kJ mol^{-1} Binaries Eq. [11]	$\Delta_{mix}H$, kJ mol^{-1} Binaries Exp. Data
AlCoCrCuFeNi	− 7.33	− 11.65
AlCoCuFeNi	− 8.50	− 16.01
CoCrCuFeNi	3.71	2.74
AlCoCuFe	− 6.66	− 12.68
AlCoCrNi	− 19.52	− 23.90

Table III. Phase Transition Temperatures of the Investigated Alloys

Samples	Experimental Data T_L (K)	Ref. [5] T_L (K)
AlCoCrCuFeNi	1596.3 ± 0.3	1603
AlCoCuFeNi	1598 ± 0.8	—
CrCoCuFeNi	1647.8 ± 0.5	1662
AlCoCuFe	1626.1 ± 0.8	—
AlCoCrNi	1661 ± 0.4	—

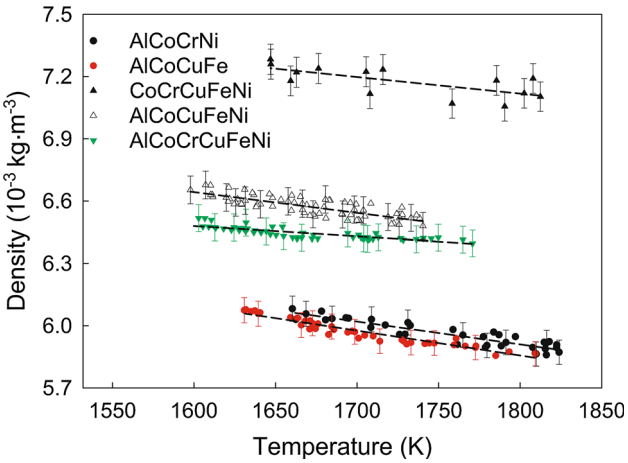

Fig. 1—Temperature dependence of density of multi-component Al-Co-Cr-Cu-Fe-Ni alloys.

CrFeNi solution calculated considering the binary excess parameters of the excess volume (ternary interaction parameter was assumed to be zero)[9] and of the liquid CuFeNi solution taking into account binary and ternary interaction parameters[10] are equal to + 0.17 × 10^{-6} and + 0.40 × 10^{-6} mol^{-1}, respectively. Therefore, the volume changes in the CoCrCuFeNi melt correspond to the overall trend of solid solutions in the liquid state.

In the following, it will be discussed whether the presence of Al in the investigated multi-component alloys may lead to the formation of a short-range order with heterocoordination in the liquid and whether and how this is expressed by a negative excess volume.

The negative values of $\Delta_{mix}H$ correspond to preferred interactions between unlike atoms and a formation of regions with a short-range order dominated by heterocoordination in the liquid, while the positive values are inherent to systems with a tendency to demixing. Due to this fact, it is often tacitly assumed that system with preferred interactions between unlike atoms also exhibit a negative excess volume while, vice versa, systems with a tendency to demixing tend to exhibit a positive excess volume. This has systematically been investigated by M. Watanabe *et al.*[49] and Brillo.[7,10,47] It is evident from these investigations that such a correlation between V^E and $\Delta_{mix}H$ exists as a rough trend, only. In particular, there are also a number of exceptions. For instance, positive values of the excess volume were declared for Cu-Ti[50] and In-Sb.[51] Both are compound-forming systems, while Cu-Ni[47] and Co-Cu-Ni,[47] both solid solution systems, exhibit negative values of V^E. Hence, it is not clear *a priori*, if a relation between V^E and $\Delta_{mix}H$ can be established for the systems of the present work or not.

Table IV. Parameters ρ_L and ρ_T, of the Linear Fits of Eq. [13] to the Experimental Density for Liquid HEA

Alloy Composition	T_L (K)	ρ_L (10^{-3} kg m^{-3})	ρ_T (10^{-4} K^{-1})
AlCoCrCuFeNi	1598 ± 2	6.481 ± 0.104	− 0.015 ± 0.001
AlCoCuFeNi	1598 ± 1	6.645 ± 0.110	− 0.010 ± 0.001
CoCrCuFeNi	1647 ± 1	7.240 ± 0.151	− 0.008 ± 0.002
AlCoCuFe	1629 ± 2	6.062 ± 0.101	− 0.012 ± 0.001
AlCoCrNi	1660 ± 1	6.064 ± 0.099	− 0.011 ± 0.001

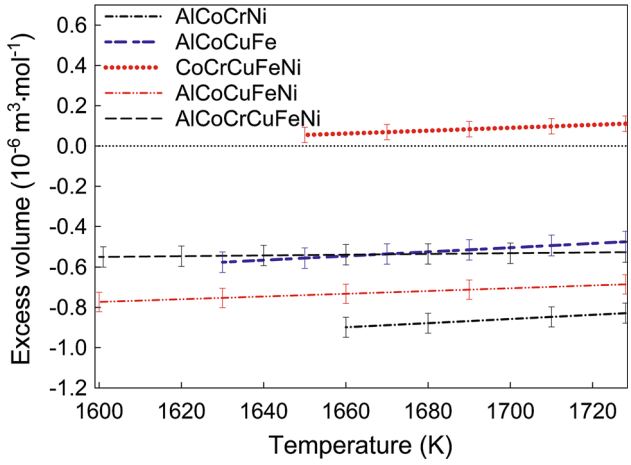

Fig. 2—Temperature dependence of the excess molar volume of multi-component Al-Co-Cr-Cu-Fe-Ni alloys.

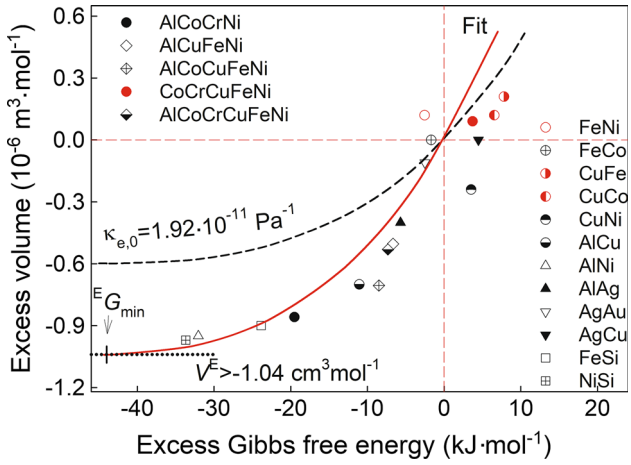

Fig. 3—Maximum excess volume of the high-entropy Al-Co-Cr-Cu-Fe-Ni alloys *vs* their estimated excess free energy calculated by Eq. [2] and by assuming that ${}^{E}G \approx \Delta_{mix}H$ at 1700 K. The plot also shows data for binary systems taken from Ref. [9]. The solid line is a fit of Eq. [16] to all data and the dashed line is calculated from the same equation by assuming $\kappa_{e,0} = 1.92 \times 10^{-11}$ Pa^{-1}.

Figure 3 shows a plot of the excess volumes obtained for the systems investigated in the present work at 1700 K *vs* their estimated excess free energies ${}^{E}G$. This is done in order to be able to compare the data with the model outlined below and available literature data shown in the figure as well. As no information on the excess entropy ${}^{E}S$ is available for these systems and as the latter is usually very small, it is justified to neglect ${}^{E}S$ and estimate ${}^{E}G$ from the integral enthalpies of mixing calculated by Kohler's model at 1700 K, *i.e.*, ${}^{E}G \approx \Delta_{mix}H$. Obviously, V^E correlates with $\Delta_{mix}H$ and, hence also with ${}^{E}G$, where positive values of V^E correspond to positive values of ${}^{E}G$ and negative values of V^E correspond to negative values of ${}^{E}G$, too.

It seems as indicated from the left-hand side of the diagram that V^E would tend against a limit when ${}^{E}G$ converges towards $-\infty$, *i.e.*, $|V^E| < 1.04$ for ${}^{E}G \rightarrow -\infty$. A curve through all data points has a concave shape. In Figure 3, negative excess volumes are much more pronounced than positive ones. While the systems for which $V^E < 0$, *i.e.,* AlCoCrNi, AlCoCuFeNi, AlCoCrCuFeNi, and AlCuFeNi exhibit excess volumes in the range of $0.4 < |V^E| < 1.0$, the excess volume of the CoCuCrFeNi system, which is positive, is much closer to zero, *i.e.*, $0.0 < |V^E| < 0.1$.

Qualitatively, the same result is empirically found by Watanabe *et al.*[49] by plotting the maximum of the excess volumes of various binary alloys *vs* the corresponding maxima of their excess free energies. This is also shown in Figure 3. Obviously, all data lie on the same curve.

We actually observed that his relation between V^E and ${}^{E}G$ is also valid for the systems investigated in the present work. A model producing a curve through all points in Figure 3 would hence reveal a fundamental mechanism valid as a trend for all systems. Insights on how an excess volume is generated in an Al-based alloy come from our earlier investigation on Al-Au.[52] In this work, it has been concluded by using the molecular dynamics (MD) technique that the huge negative excess volume evident in this system originates from the formation of compact aggregates with tetrahedral chemical short-range order combined with a "compression" of the less dense Al matrix when Au atoms are added. This mechanism is probably of general validity for Al-based melts.

If we consider only the compression effect, a simple thermodynamic relation can be formulated between the excess volume and the excess free energy. For this purpose, it is assumed that addition of a macroscopic amount of alien atoms to a matrix, *e.g.*, Al, may cause an inner tension in the matrix which can be represented by an effective internal pressure $\tilde{P}$. If this internal pressure is directed outwards, an expansion of the volume may be the consequence.

If, due to attractive forces, caused for instance by bond-hybridization, $\tilde{P}$ is directed inwards, the volume is compressed. Hence, one can define an effective compressibility κ_e:

$$\kappa_e = +\frac{1}{V}\frac{\partial V}{\partial \tilde{P}}. \quad [11]$$

Formally, Eq. [11] is the same as the definition of the isothermal compressibility, except that the meaning of the pressure is different and that the minus sign is omitted. It is easily seen by multiplying both sides by $V = {}^{id}V + V^E$, where ${}^{id}V$ is the volume of the ideal solution, that Eq. [11] also holds for the excess volume V^E:

$$V^E \cdot \kappa_e({}^E G) = \frac{\partial {}^E G}{\partial \tilde{P}} \cdot \kappa_e({}^E G) = \frac{\partial V^E}{\partial \tilde{P}}. \quad [12]$$

It is used in Eq. [12] that the excess volume can be obtained by differentiation from the excess free energy ${}^E G$. Moreover, it is allowed in Eq. [12] that κ_e is a function of ${}^E G$. To the first degree of approximation, this function would be linear in ${}^E G$:

$$\kappa_e({}^E G) \approx \kappa_{e,0} + \kappa_{e,1}{}^E G, \quad [13]$$

where $\kappa_{e,0}$ denotes the effective compressibility of the corresponding ideal solution and $\kappa_{e,1}$ denotes the linear coefficient. It takes into account that the stiffness of the matrix might be affected by attractive or repulsive interactions between unlike atoms. Combining Eqs. [12] and [13] yields

$$\kappa_{e,0}\frac{\partial {}^E G}{\partial \tilde{P}} + \kappa_{e,1}{}^E G\frac{\partial {}^E G}{\partial \tilde{P}} \approx \frac{\partial V^{Ex}}{\partial \tilde{P}}. \quad [14]$$

The pressure is eliminated by integration of Eq. [14]:

$$\left[\kappa_{e,0}{}^E G + \frac{1}{2}\kappa_{e,1}{}^E G^2\right] \approx V^{Ex}. \quad [15]$$

In principle, Eq. [15] is the desired relation. However, it is beneficial for the following discussion to further transform the expression. In particular, the linear approximation can be expanded into an exponential and the ratio of $\kappa_{e,0}$ to $\kappa_{e,1}$ is abbreviated as λ/PT:

$$V^E \approx 2\kappa_{e,0}{}^E G \exp\left(\lambda\frac{{}^E G}{RT}\right). \quad [16]$$

In reality, this relation is not necessarily true for each system. Cu-Ti, for instance, has a negative free energy of mixing and a strong positive excess volume.[50] This would contradict Eq. [16]. Moreover, it was shown theoretically that every combination of the signs of ${}^E G$ and V^E is possible.[53] However, Eq. [16] may be true on an average scale for a number of systems which we want to declare as "normal" or "benign" systems. Equation [16] has the following properties: the excess volume of an ideal solution is zero, *i.e.*, $V^E = 0$ for ${}^E G = 0$. In fact, the integration constant is chosen such in Eq. [14] that this property is fulfilled. Moreover, V^E monotonically increases with increasing ${}^E G$ and deviates from the linear law for strongly non-ideal systems, *i.e.*, where ${}^E G \ll 0$. These features are also observed in the experimental data in Figure 3.

Mathematically, Eq. [16] exhibits a minimum at ${}^E G = {}^E G_{min}$ where ${}^E G_{min}$ is obtained as

$${}^E G_{min} = -\frac{RT}{\lambda}. \quad [17]$$

On the other hand, the internal energy $U = 3RT$ is a lower limit for ${}^E G$ if it is assumed that in addition to translations also a rotational degree of freedom exists. This holds at least as an approximation, as the excess entropy was neglected. Hence, it follows from Eq. [17] that

$$\lambda = \frac{1}{3}. \quad [18]$$

As a consequence of Eq. [18], a lower boundary for the excess volume follows, which generally depends on temperature. This dependency, however, should be very weak, as most systems are studied in the same temperature range. In the case of 1700 K, the limit is 1.04 (10^{-3} m^3 mol^{-1}), *i.e.*,

$$V^E \geq -1.04(10^{-3}\mathrm{m}^3 \cdot \mathrm{mol}^{-1}). \quad [19]$$

As visible in Figure 3, this limit is nearly reached experimentally.

In order to discuss Eq. [15], the parameter $\kappa_{e,0}$ is considered constant and independent of composition. This means that it is the same for all systems and represents an effective mean value.

Table V lists the isothermal compressibility factors κ_T for some pure elements which are calculated from ultrasound velocities, densities, and specific heats listed in References 54 through 56.

As a first guess, $\kappa_{e,0}$ is set equal to the mean of the isothermal compressibilities of the elements Al, Co, Cu, Fe, and Ni, which amounts to 1.92×10^{-11} Pa^{-1}, see Table V. As a result, the dashed line is obtained in Figure 3 which already gives a good estimate of the order of magnitude and the qualitative shape of the

Table V. Isothermal Compressibility at 1700 K Calculated from Parameters Listed in Refs. [54, 56] for Some Pure Elements and Their Mean Value

Element	κ_T (10^{-11} Pa^{-1})
Al	3.19
Co	1.64
Cu	1.32
Ni	1.97
Fe	1.47
Mean	1.92

curve. However, the experimental findings are overestimated by nearly 50 pct.

A fit of Eq. [16] to all data shown in Figure 3 yields $\kappa_{e,0} = 3.2 \times 10^{-11}$ Pa^{-1} which is strikingly close to the isothermal compressibility of pure Al which is 3.19×10^{-11} Pa^{-1}, see Table V.

This finding makes sense in the view of the mechanism proposed in Reference 52, namely that the excess volume is generated by compression of the Al-nearest neighbor bonds. Hence, the compressibility of Al should play a key role in Eq. [16]—which it does. However, the same fit also applies to systems in Figure 3, which do not contain any Al at all, such as Fe-Si. This may indicate that the value of 3.2×10^{-11} Pa^{-1} is of more general validity. For instance, it is conceivable that less dense metallic liquid systems, like Al, Si, or others, also have similar values in $\kappa_{e,0}$.

A second look at Figure 3 shows, however, that the data for the high-entropy alloys studied in the present work is still slightly overestimated by the fit of Eq. [16]. One can argue that this small discrepancy is due to an experimental uncertainty which is of the same order of magnitude. However, this discrepancy is common to the data of nearly all Al-based systems presented in Figure 3. This brings us back to the second cause of the excess volume, discussed in Reference 52, namely, the formation of compact tetrahedral aggregates in the melt, which can further reduce the volume. The formation of such aggregates or compounds would therefore also take place in the liquid high-entropy alloys, except CoCrCuFeNi. A preferred interaction between unlike atoms can be supposed hereby.

V. CONCLUSIONS

The densities of the liquid high-entropy alloys AlCoCrCuFeNi, AlCoCuFeNi, and CrCoCuFeNi, as well as quaternary liquid AlCoCuFe and AlCoCrNi alloys have been determined over a wide temperature range by a non-contact technique combining electromagnetic levitation and optical dilatometry. The liquidus temperatures for the investigated multi-component alloys were determined by DTA analysis. The obtained excess volumes are as function of the excess free energies estimated from Kohler's model follow a general trend, which is explained by using a simple model as a compression effect of the less dense Al matrix in these systems. In these melts, the interactions between the unlike atoms prevail, while in the CrCoCuFeNi alloy the preferred interactions between similar atoms are expected. In this manner, two basic effects, namely, compression of the Al-nearest neighbor bonds and formation of short-range order affect the excess volume in multi-component high-entropy alloys containing aluminum. In was revealed that in most investigated multi-component alloys, the excess molar volume decreases with the increasing number of the alloy components.

ACKNOWLEDGMENTS

The authors acknowledge the support of this work by the German Aerospace Center (DLR) and the German Academic Exchange Service (DAAD) under DLR-DAAD Research Fellowship No. 252 (Yu. Plevachuk and J. Brillo), and by the Austrian Science Fund (FWF) under Project No. P27049 (A. Yakymovych).

REFERENCES

1. K.H. Huang: *A Study on the Multicomponent Alloy Systems Containing Equal-Mole Elements*, National Tsing Hua University, Hsinchu City, Taiwan, 1996.
2. J.W. Yeh, S.K. Chen, S.J. Lin, J.Y. Gan, T.S. Chin, T.T. Shun, C.H. Tsau, and S.Y. Chang: *Adv. Eng. Mater.*, 2004, vol. 6, pp. 299–303.
3. D.B. Miracle and O.N. Senkov: *Acta Mater.*, 2017, vol. 122, pp. 448–511.
4. M.H. Tsai and J.W. Yeh: *Mater. Res. Lett.*, 2014, vol. 2, pp. 107–23.
5. C.J. Tong, Y.L. Chen, S.K. Chen, J.W. Yeh, T.T. Shun, C.H. Tsau, S.J. Lin, and S.Y. Chang: *Metall. Mater. Trans. A*, 2005, vol. 36A, pp. 881–93.
6. M.H. Chuang, M.H. Tsai, W.R. Wang, S.J. Lin, and J.W. Yeh: *Acta Mater.*, 2011, vol. 59, pp. 6308–17.
7. J. Brillo: *Thermophysical Properties of Multicomponent Liquid Alloys*, De Gruyter, Oldenbourg, 2016.
8. J. Brillo and I. Egry: *Jpn. J. Appl. Phys.*, 2011, vol. 50, p. 11RD02.
9. H. Kobatake and J. Brillo: *J. Mater. Sci.*, 2013, vol. 48, pp. 6818–24.
10. J. Brillo, I. Egry, and T. Matsushita: *Int. J. Thermophys.*, 2006, vol. 27, pp. 1778–91.
11. A.R. Miedema, F.R. Deboer, and R. Boom: *Physica B & C*, 1981, vol. 103, pp. 67–81.
12. D.M. Herlach, R.F. Cochrane, I. Egry, H.J. Fecht, and A.L. Greer: *Int. Mater. Rev.*, 1993, vol. 38, pp. 273–347.
13. J. Brillo and I. Egry: *Int. J. Thermophys.*, 2003, vol. 24, pp. 1155–70.
14. L.J. Gallego, J.A. Somoza, and J.A. Alonso: *J. Phys. Condens. Mater.*, 1990, vol. 2, pp. 6245–50.
15. P.K. Ray, M. Akinc, and M.J. Kramer: *J. Alloys Compd.*, 2010, vol. 489, pp. 357–61.
16. S. Bera, S. Mazumdar, M. Ramgopal, S. Bhattacharyya, and I. Manna: *J. Mater. Sci.*, 2007, vol. 42, pp. 3645–50.
17. T.X. Fan, G. Yang, and D. Zhang: *Mater. Sci. Eng. A*, 2005, vol. 394, pp. 327–38.
18. J.F. Herbst: *J. Alloys Compd.*, 2002, vol. 337, pp. 99–107.
19. B.W. Zhang and W.A. Jesser: *Physica B*, 2002, vol. 315, pp. 123–32.
20. A.P. Goncalves and M. Almeida: *Physica B*, 1996, vol. 228, pp. 289–94.
21. R.F. Zhang, S.H. Zhang, Z.J. He, J. Jing, and S.H. Sheng: *Comput. Phys. Commun.*, 2016, vol. 209, pp. 58–69.
22. F. Kohler: *Chem. Montly*, 1960, vol. 91, pp. 738–40.
23. A.R. Miedema, A.K. Niessen, F.R. de Boer, R. Boom, and W.C.M. Mattens: *Cohesion in Metals: Transition Metal Alloys*, North-Holland, Amsterdam, 1988.
24. A.R. Miedema, P.F. Dechatel, and F.R. Deboer: *Physica B & C*, 1980, vol. 100, pp. 1–28.
25. M.J. Assael, K. Kakosimos, R.M. Banish, J. Brillo, I. Egry, R. Brooks, P.N. Quested, K.C. Mills, A. Nagashima, Y. Sato, and W.A. Wakeham: *J. Phys. Chem. Ref. Data*, 2006, vol. 35, pp. 285–300.
26. M.J. Assael, A.E. Kalyva, K.D. Antoniadis, R.M. Banish, I. Egry, J.T. Wu, E. Kaschnitz, and W.A. Wakeham: *High Temp. High Press.*, 2012, vol. 41, pp. 161–84.
27. M.J. Assael, A.E. Kalyva, K.D. Antoniadis, R.M. Banish, I. Egry, J.T. Wu, E. Kaschnitz, and W.A. Wakeham: *J. Phys. Chem. Ref. Data*, 2010, vol. 39, p. 033105.

28. F. Xiao: *J. Mater. Sci. Technol.*, 2003, vol. 19, pp. 16–18.
29. J. Havrankova, J. Vrestal, and J. Tomiska: *Kovove Mater.*, 1999, vol. 37, pp. 34–41.
30. M.A. Turchanin: *Powder Metall. Met. C*, 2006, vol. 45, pp. 457–67.
31. M.A. Turchanin and I.V. Nikolaenko: *J. Alloys Compd.*, 1996, vol. 235, pp. 128–32.
32. M.A. Shevchenko, V.V. Berezutskii, M.I. Ivanov, V.G. Kudin, and V.S. Sudavtsova: *Russ. J. Phys. Chem. A*, 2014, vol. 88, pp. 729–34.
33. P. Saltykov, V.T. Witusiewicz, I. Arpshofen, H.J. Seifert, and F. Aldinger: *J. Mater. Sci. Technol.*, 2002, vol. 18, pp. 167–70.
34. V.T. Witusiewicz, U. Hecht, S.G. Fries, and S. Rex: *J. Alloy Compd.*, 2004, vol. 385, pp. 133–43.
35. G.I. Batalin, E.A. Beloborodova, and V.P. Kazimirov: *Termodinamika i stroenie zhidkikh splavov na osnove aliuminiia*, Metallurgiia, Moskva, 1983.
36. N.V. Gizenko, S.N. Kilesso, D.V. Ilinkov, B.J. Emlin, and A.L. Zavyalov: Izv. Akad. Nauk SSSR Zvetnyje*Metally*, 1983, vol. 4, pp. 21–24.
37. I.V. Nikolaenko and M.A. Turchanin: *Metall. Mater. Trans. B*, 1997, vol. 28B, pp. 1119–30.
38. B. Predel and R. Mohs: *Arch. Eisenhuttenwes.*, 1970, vol. 41, pp. 143–49.
39. B. Predel and R. Mohs: *Arch. Eisenhuttenwes.*, 1970, vol. 41, pp. 61–66.
40. G.I. Batalin, V.P. Kurach, and V.S. Sudavtsova: *Zh. Fiz. Khim.*, 1984, vol. 58, pp. 481–83.
41. Y. Iguchi, S. Nobori, K. Saito, and T. Fuwa: *Trans. Iron Steel Inst. Jpn.*, 1982, vol. 68, pp. 633–40.
42. A. Khasan, K. Abdel-Aziz, A.A. Vertman, and A.M. Samarin: Izv. Akad. Nauk SSSR*Metally*, 1966, vol. 3, pp. 19–30.
43. M.A. Turchanin: *Russ. Metally*, 1995, vol. 5, pp. 12–19.
44. X. Yang and Y. Zhang: *Mater. Chem. Phys.*, 2012, vol. 132, pp. 233–38.
45. S. Guo and C.T. Liu: *Prog. Nat. Sci. Mater.*, 2011, vol. 21, pp. 433–46.
46. H. Arslan and A. Dogan: *Russ. J. Phys. Chem. A*, 2016, vol. 90, pp. 2339–45.
47. J. Brillo and I. Egry: *Z. Metallkd.*, 2004, vol. 95, pp. 691–97.
48. L. Vegard: *Z. Phys.*, 1921, vol. 5, pp. 17–26.
49. M. Watanabe, M. Adachi, and H. Fukuyama: *J. Mater. Sci.*, 2016, vol. 51, pp. 3303–10.
50. S. Amore, S. Delsante, H. Kobatake, and J. Brillo: *J. Chem. Phys.*, 2013, vol. 139, p. 064504.
51. A.R. Hansen, M.A. Kaminski, and C.A. Eckert: *J. Chem. Eng. Data*, 1990, vol. 35, pp. 153–56.
52. H.L. Peng, T. Voigtmann, G. Kolland, H. Kobatake, and J. Brillo: *Phys. Rev. B*, 2015, vol. 92, p. 184201.
53. S. Amore, J. Horbach, and I. Egry: *J. Chem. Phys.*, 2011, vol. 134, p. 044515.
54. M. Leitner, T. Leitner, A. Schmon, K. Aziz, and G. Pottlacher: *Metall. Mater. Trans. A*, 2017, vol. 48A, pp. 3036–45.
55. G. Pottlacher: *High Temperature Thermophysical Properties of 22 Pure Metals*, Edition Keiper, Graz, Austria, 2010.
56. J. Kawai and J. Shiraishi: *Handbook of Physico-chemical Properties at High Temperatures*, The Iron and Steel Institute of Japan, Tokyo, Japan, 1988.